In Silico Evaluation of YCT-529:

Pharmacokinetics, ADME Properties, and Clinical Implications for Male Contraception

Capstone Project

Praise Ogwuche

Advisor: Prof. Stan

Minerva University

Submitted: April 5, 2025

Contents

Abstract

This study employs physiologically based pharmacokinetic (PBPK) modeling to characterize the pharmacokinetics of YCT-529, a non-hormonal male contraceptive, across diverse populations and dosing regimens. Using PK-Sim, a PBPK/PD modeling platform for simulating drug absorption, distribution, metabolism, and excretion, and ADMETLab 3.0, a cheminformatics tool that predicts physicochemical, ADME, and toxicity properties using machine learning, simulations were conducted in 4,000 participants (1,000 each of Black Americans, East Asians, White Americans, and Europeans) at four doses (15 mg, 45 mg, 90 mg, and 180 mg). A control compound was also modeled, resulting in a total of 16,000 simulations. Additionally, Atazanavir, a CYP3A4-metabolized reference drug, was simulated in 1,000 individuals to validate the modeling approach.

YCT-529 exhibited rapid absorption, with $T_{\max}$ occurring within 1–3 hours and dose-dependent increases in systemic exposure, reaching $C_{\max}$ values of 50 µg/L at 15 mg and 500 µg/L at 180 mg. East Asians demonstrated the highest systemic retention ($C_{\max}$ 500 µg/L at 180 mg), while Black Americans had the lowest (300 µg/L), consistent with known metabolic variability of CYP3A4. Dietary intake significantly influenced systemic exposure, as fasting increased $C_{\max}$ to a mean of 45.85 µg/L while high-fat meals reduced it to 28.32 µg/L. Statistical analysis confirmed significant differences in $C_{\max}$ across dietary conditions (ANOVA $F = 793.45$, $p < 0.001$), with large effect sizes between fasted vs. light meal ($d = 1.38$, $p < 0.001$) and fasted vs. high-fat breakfast ($d = 1.61$, $p < 0.001$); no significant differences were observed between the light meal and high-fat breakfast groups ($d = 0.22$, $p = 0.842$). The predicted pharmacokinetics of Atazanavir closely mirrored clinical data, supporting the validity of the simulations. Limitations include sociological acceptance of an oral male contraceptive, reliance on computational models without experimental validation, necessitating further in vivo studies to refine dosing regimens and confirm findings. These results highlight the utility of PBPK modeling in optimizing contraceptive pharmacotherapy, guiding clinical trial design, and tailoring treatment strategies based on population-specific pharmacokinetics.

Keywords: YCT-529, pharmacokinetics, PBPK modeling, non-hormonal male contraceptive, PK-Sim, ADMETLab, population-specific pharmacokinetics, contraceptive pharmacotherapy, CYP3A4 metabolism

Introduction

Background

YCT-529 represents a significant advancement in the field of male contraceptives, offering a novel, non-hormonal mechanism of action. Unlike traditional hormonal contraceptives, which modulate the endocrine system and are often associated with adverse side effects, YCT-529 operates through a targeted, non-hormonal pathway. As noted in prior review, YCT-529 inhibits key biological processes essential for spermatogenesis, positioning it as a promising alternative for male contraception [33, 34]. However, understanding its pharmacokinetics - specifically how it behaves once administered - is critical for further clinical development.

Research Context

Research on YCT-529 remains limited due to proprietary restrictions on preclinical and clinical data. Despite its progression to clinical trials, comprehensive datasets on its ADME properties and pharmacokinetics remain unavailable until publication by Communications Medicine. This lack of empirical data hinders precise predictions regarding safety, efficacy, and dosing. As highlighted by Kimmelman et al. [22], computational modeling and theoretical frameworks become essential in addressing these knowledge gaps, enabling preliminary pharmacokinetic assessments. Without direct experimental validation, exploratory methodologies serve as a crucial tool for understanding YCT-529's metabolism, systemic distribution, and potential therapeutic applications.

In the absence of direct experimental data, alternative approaches become essential for informed discovery. Physiologically based pharmacokinetic (PBPK) models offer a powerful method to simulate YCT-529's behavior in silico, integrating molecular descriptors, physiological variables, and population-specific factors to predict pharmacokinetics. Tools like PK-Sim facilitate plasma concentration predictions and metabolic pathway identification, forming a basis for hypothesis generation. As Edginton et al. [13] demonstrated, PBPK models effectively address knowledge gaps in data-limited scenarios, making exploratory research critical for characterizing YCT-529's therapeutic profile and guiding confirmatory clinical studies.

Research Question

The research question, *How can computational pharmacokinetic modeling provide preliminary insights into the ADME properties of YCT-529?*, is critical for addressing knowledge gaps in YCT-529's pharmacokinetics without experimental data. Using computational tools such as SMILES generators, ADMETLab, and PK-Sim, this study simulates key

ADME processes to predict drug behavior. Comparisons with a placebo, microcrystalline cellulose (MCC), and Atazanavir as a validation reference provide essential context for absorption, distribution, and metabolism. These insights inform dosage optimization, predict drug interactions, and guide clinical trial designs, demonstrating the utility of computational pharmacokinetics in evaluating novel contraceptives.

Objectives

This study aims to analyze the pharmacokinetics of YCT-529 using computational models, addressing the lack of empirical data and providing preliminary ADME insights. The key objectives are:

- Pharmacokinetic Modeling: Simulate in-silico clinical trials using PK-Sim to predict YCT-529's bioavailability, dosage requirements, and metabolic pathways.
- Comparative Analysis: Evaluate YCT-529 against a placebo (microcrystalline cellulose) and Atazanavir to validate results and contextualize absorption, distribution, and metabolism.
- Optimization and Validation: Guide dosage planning, assess computational modeling limitations, and provide a foundation for future clinical studies.

Achieving these objectives advances the understanding of YCT-529's pharmacokinetics and its potential as a non-hormonal male contraceptive.

Methodology

I followed a structured computational workflow to simulate YCT-529's pharmacokinetics using PBPK modeling tools (see Figure 1). I generated the SMILES string, predicted physicochemical properties via ADMETLab [24], and modeled ADME behavior in PK-Sim [44]. To validate my results, I compared YCT-529 against microcrystalline cellulose (MCC) as a placebo [3, 39] and Atazanavir as a reference drug [2]. I selected PK-Sim over BioGears [8] due to its user-friendly interface, physiologically realistic models, and robust PBPK capabilities. This methodology allowed me to generate accurate pharmacokinetic predictions, analyze absorption, distribution, metabolism, and excretion, and establish a validated baseline through placebo and reference drug comparisons.

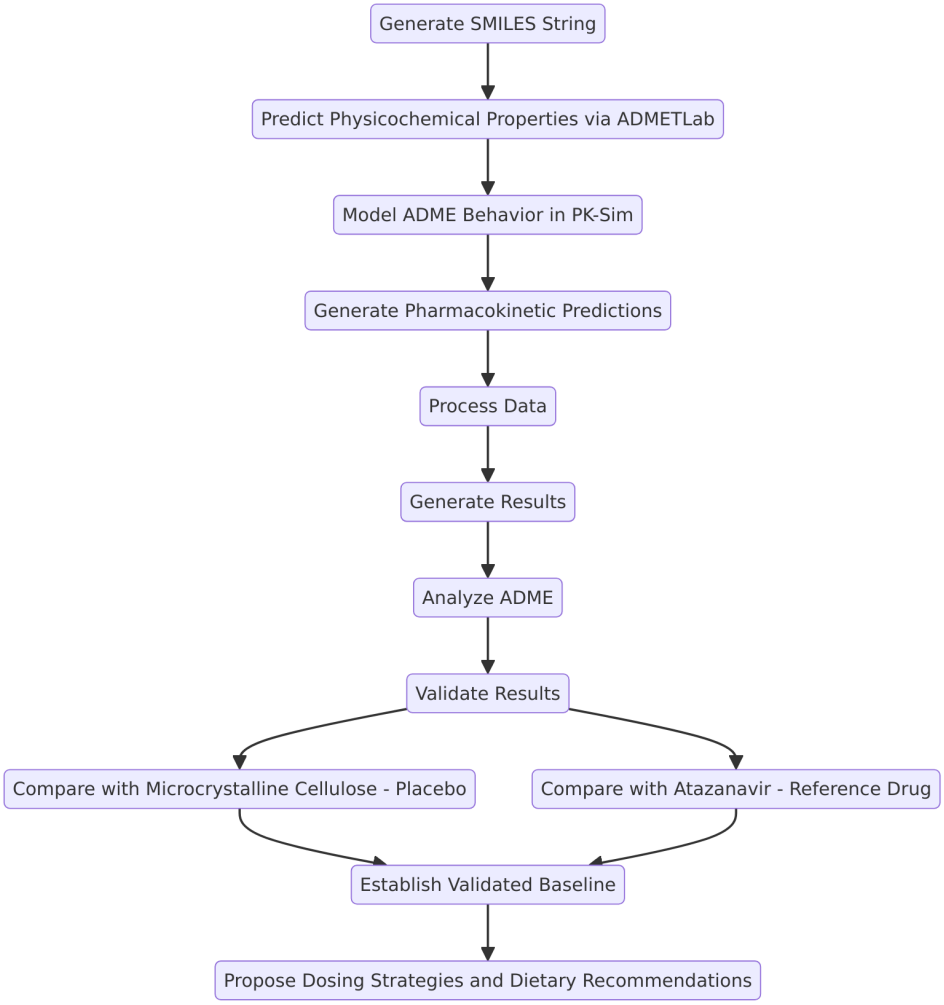

Figure 1: *Sequential computational workflow for modeling YCT-529's pharmacokinetics. The workflow includes molecular structure generation, ADMET property prediction, PBPK modeling in PK-Sim, result analysis, and validation using a placebo (MCC) and a reference drug (Atazanavir).*

SMILES String Generation

The first step in the computational workflow for analyzing YCT-529 involved using the SMILES generator available at Cheminfo.org [10]. SMILES (Simplified Molecular Input Line Entry System) is a text-based notation that encodes a molecule's structure into a single line of ASCII characters. This step is essential because SMILES provides the standardized molecular representation required by cheminformatics tools like ADMETLab and PK-Sim to perform accurate property predictions and pharmacokinetic simulations. So, I replicated the structure of YCT-529 with high precision referencing the molecular structure provided by the PubChem database [29].

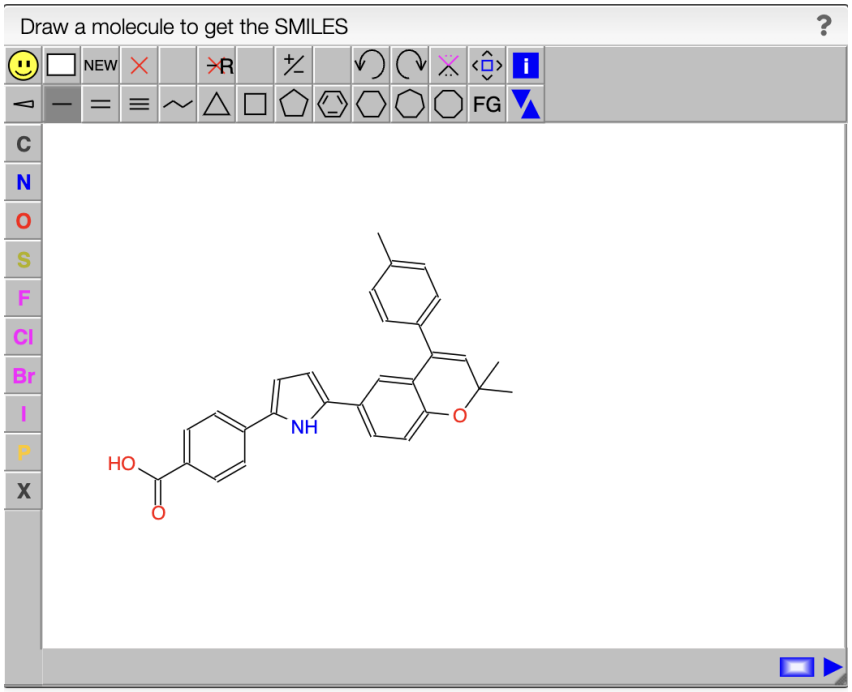

Figure 2: *Structure of YCT-529 constructed using the JSME molecular editor on Cheminfo.org for SMILES string generation, illustrating the compound's key functional groups and molecular framework [10].*

The SMILES string generated for YCT-529 was:

`Cc5ccc(C3=CC(C)(C)Oc4ccc(c2ccc(c1ccc(C(=O)O)cc1)[nH]2)cc34)cc5`.

I verified the SMILES string using Chemaxon, a chemical sketch tool by the RCSB Protein Data Bank (PDB), which provides access to 3D molecular structure data for biological and chemical research [15]. I loaded the generated SMILES string to visualize its molecular structure (Figure 3). The resulting structure matched the known reference for YCT-529, confirming the validity of the string. For MCC, I retrieved the D-glucose SMILES from PubChem [29], ensuring precision and facilitating its integration into subsequent computational analyses.

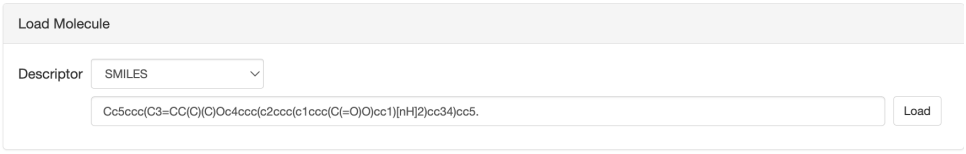

(a) SMILES string inputted into ChemAxon using the Load Molecule interface.

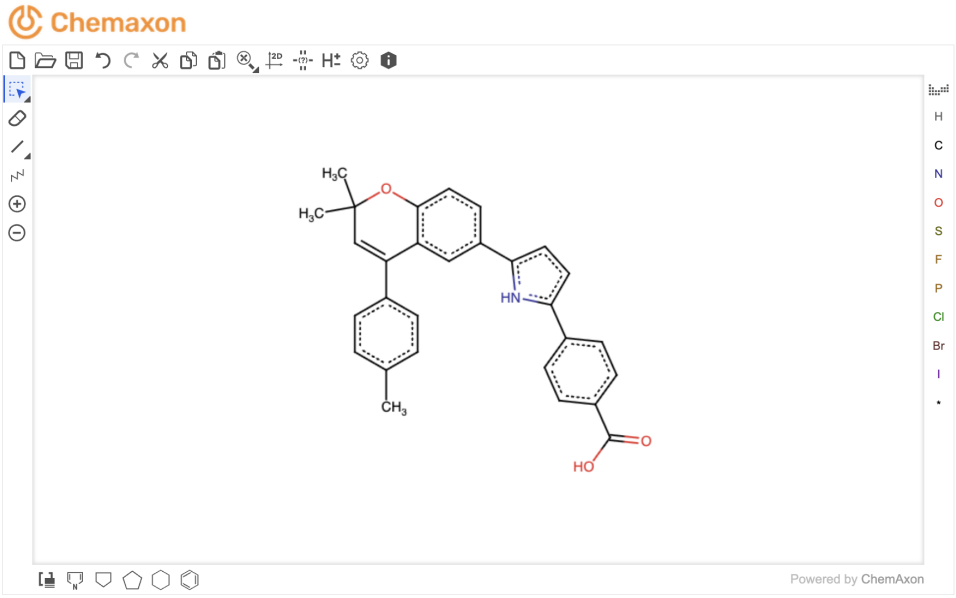

(b) Chemical structure generated by ChemAxon after loading the SMILES string for YCT-529.

Figure 3: *Verification of YCT-529's SMILES string using ChemAxon, a chemical sketch tool maintained by RCSB PDB, the U.S. data center for the global Protein Data Bank. The structure output confirmed fidelity to the molecular framework referenced from PubChem.*

ADMETLab 3.0 Analysis

After generating the SMILES string for YCT-529, I analyzed the compound using ADMETLab 3.0, a cheminformatics platform that evaluates physicochemical, medicinal chemistry, ADME, and toxicity properties. The physicochemical properties, all enumerated in Appendix ϕ, included molecular weight (435.18 g/mol), LogP (5.706), LogS (-5.761), and TPSA (62.32 Å^2), alongside density (0.925 g/cm^3) and flexibility (0.138). The high LogP value of 5.706 suggests strong lipophilicity, enhancing membrane permeability but potentially limiting solubility [25]. This aligns with the LogS value of -5.761, corresponding to a solubility of approximately 0.067 mg/mL, which may hinder gastrointestinal dissolution. The TPSA of 62.32 Å^2 suggests moderate polarity, supporting passive diffusion while maintaining sufficient hydrophilicity for receptor binding. ADMETLab confirmed that YCT-529 adheres to Lipinski's Rule of Five, which evaluates molecular weight, hydrogen bond donors/acceptors, and lipophilicity. Compliance with this rule indicates favorable absorption and permeability when administered orally [25]. However, the rejection of the GSK rule, which considers solubility and synthetic

feasibility, suggests potential challenges in manufacturing and ADMET liabilities, such as toxicity risks [18]. This was reflected in toxicity predictions, which indicated high risks for drug-induced liver injury (DILI: 0.998) and genotoxicity (0.983). Despite these concerns, ADMETLab's machine-learning algorithms generate reliable predictions, supporting the exploratory nature of this research [50].

To establish a baseline comparison, I selected microcrystalline cellulose (MCC) as the placebo due to its well-documented inert and non-absorbable properties in pharmaceutical formulations [39, 3]. MCC is a polymer composed of glucose monomers, making it hydrophilic but non-ionizable, with an approximated LogP of 0. The molecular weight of MCC (180.06 g/mol) is equivalent to its monomeric unit, D-glucose, which has a LogP of -2.229, confirming its hydrophilic nature and inability to partition into lipid bilayers. The solubility of D-glucose (LogS 0.339) is significantly higher than MCC's near-insolubility (<0.01 g/L), reflecting the reduced water solubility caused by polymerization. Additionally, MCC exhibits negligible plasma protein binding or metabolic activity, making it pharmacologically inactive and ideal as a placebo for comparative pharmacokinetic modeling. These insights ensured MCC's accurate representation in PK-Sim, allowing for a meaningful evaluation of YCT-529's pharmacokinetic properties.

Building the Pharmacokinetic Model

I used PK-Sim (Version 12.0) to construct a physiologically based pharmacokinetic (PBPK) model for YCT-529, MCC, and Atazanavir. By integrating physicochemical and ADME data from ADMETLab, I simulated absorption, distribution, metabolism, and excretion across tissues. PK-Sim's Monte Carlo simulations enabled interindividual variability modeling, supporting population-level pharmacokinetic predictions [13].

PK-Sim Overview: Etymology, Function, and Applicability

PK-Sim bridges experimental data and in silico simulations using dynamic compartmental modeling across 18 tissues [44]. Its predictive capabilities for lipophilic drugs like YCT-529 are well-documented [31]. The software successfully models retinoic acid receptor antagonists, supporting its application to YCT-529 [32], with accuracy derived from clinical and preclinical physiological datasets.

Model Development

I created my model in PK-Sim in the following steps: Individuals and Populations, Compound Creation, and Formulation and Administration Protocols.

1. Individuals and Populations: I defined the demographic and physiological characteristics of simulation subjects to reflect clinical realities and scientific rationale. Using

PK-Sim's race-specific models, I generated populations of 1000 Black American, East Asian, White American, and European males (ages 25–60, BMI 18–32 kg/m^2) for YCT-529, MCC, and Atazanavir, ensuring relevance to ongoing clinical trials (NCT06094283, NCT06542237). Ethnic differences in drug metabolism, particularly CYP2C19 and CYP2C8 polymorphisms in East Asians, influence systemic exposure and clearance [51]. Variations in enzyme expression and transporters among African and European populations further impact pharmacokinetics [43]. PK-Sim's population module randomized physiological parameters across 1000 individuals per group, generating 4000 total subjects, allowing robust inter-individual and inter-ethnic comparisons. Despite PK-Sim's limitations in modeling additional ethnic groups like africans, these populations provide a clinically grounded baseline for evaluating YCT-529's ADME properties.

2. Compound Creation: I constructed the YCT-529 model in PK-Sim by integrating key physicochemical and ADME properties. Lipophilicity, represented by a LogP of 5.706 and a $\text{LogD}_{7.4}$ of 3.356, was critical for modeling membrane permeability and tissue distribution [50, 6]. The solubility at pH 7.4 (0.29 g/L), derived from LogS (-5.761), was incorporated to reflect moderate solubility constraints. The fraction unbound (Fu = 0.537%) indicated strong plasma protein binding (98.8%), which significantly impacts distribution and clearance [34]. These parameters align with the Biopharmaceutics Drug Disposition Classification System (BDDCS), correlating lipophilicity and solubility with absorption profiles [6].

YCT-529's metabolism was primarily mediated by CYP3A4, with additional contributions from CYP2C8 and CYP2C9 for hydroxylation [41, 30]. Phase II metabolism involved glucuronidation (UGT1A1, UGT2B7) and sulfation (SULT1E1, SULT2A1), leading to renal and biliary excretion [41]. Atazanavir, metabolized by CYP3A4 and UGT1A1, served as a reference due to its similar metabolic pathways, high plasma protein binding (99%), and biliary excretion [41]. The integration of these metabolic pathways ensured that the PK-Sim model accurately represented YCT-529's pharmacokinetics, aligning with established drug metabolism principles.

3. MCC Compound Creation: The creation of the MCC model in PK-Sim was straightforward, as its physicochemical and ADME properties are well-documented in literature and pharmacopeias. MCC, a glucose polymer (PubChem CID: 5793), was assigned a molecular weight of 180.06 g/mol, accurately reflecting its monomer composition [39]. Its LogP was set to approximately 0, consistent with its hydrophilic nature and inability to partition into lipid bilayers [39]. A fraction unbound (Fu) of 1.0 was applied, as MCC does not bind plasma proteins or enter circulation [3]. With no ionizable groups, pKa values were excluded, and solubility at physiological pH (7.4) was defined as <0.01 g/L, reflecting its practical insolubility [26]. The effective molecular weight remained

180.06 g/mol due to the absence of halogens or modifications [3]. I configured PK-Sim's compound creation module to represent MCC's non-absorbable, inert properties accurately. Intestinal permeability was set to <0.001 cm/s to reflect its lack of absorption, and volume of distribution (Vd) was omitted since MCC does not enter systemic circulation. No metabolic enzymes were assigned, as MCC resists enzymatic degradation in humans. Excretion was set as fecal, ensuring its pharmacokinetic profile as a placebo remained isolated from active pharmacological effects.

4. Atazanavir Compound Creation: I incorporated Atazanavir into my PK-Sim model by directly importing its pre-constructed compound file from the Open Systems Pharmacology Suite [2]. No modifications were made to its physicochemical or ADME parameters. Atazanavir, a lipophilic drug with a LogP of 2.12 and molecular weight of 704.9 g/mol, exhibits extensive plasma protein binding (Fu = 0.14) and undergoes primary metabolism via CYP3A4, as defined in its validated PBPK model [2]. Given its established metabolism, renal excretion accounts for approximately 7% of elimination, with the remainder undergoing biliary excretion [2]. Its inclusion provides a pharmacokinetic reference for YCT-529's metabolic behavior, particularly in assessing CYP3A4-mediated metabolism and biliary clearance.

5. Formulation and Administration Protocols: I defined dosing regimens based on clinical trials evaluating single and repeat ascending oral doses of YCT-529 (NCT06094283, NCT06542237). YCT-529 was administered orally at 15 mg, 45 mg, 90 mg, and 180 mg, dissolved in simulated gastric fluid, ensuring uniform delivery across all populations. Each dose was tested across 1000 Black American, East Asian, White American, and European males, resulting in 16 simulations (4 races $\times$ 4 doses). Similarly, microcrystalline cellulose (MCC) was administered at identical doses in simulated gastric fluid as a placebo to isolate the pharmacokinetic effects of YCT-529, leading to an additional 16 simulations. All simulations were conducted under a light meal dietary condition to ensure consistency in absorption parameters. For Atazanavir, I implemented a single-dose 400 mg oral capsule regimen across the same population (1000 individuals per race) using PK-Sim's predefined compound file [2]. This allowed comparative pharmacokinetic profiling, particularly in evaluating CYP3A4-mediated metabolism and biliary excretion. I configured PK-Sim to simulate each dosing scenario, capturing pharmacokinetic parameters such as C_{max}, T_{max}, and AUC for YCT-529, MCC, and Atazanavir. The results were exported to Google Spreadsheets for aggregation and further analysis. This methodology, while robust, could be enhanced by expanding the placebo group to refine interindividual variability and baseline pharmacokinetics further.

Model Analysis

Blood plasma concentration (C_p), specifically venous plasma concentration, is a key pharmacokinetic (PK) parameter that quantifies the amount of drug present in plasma at a given time. PK-Sim models venous rather than arterial plasma concentrations because venous blood represents post-capillary circulation, reflecting the net effect of absorption, distribution, metabolism, and excretion (ADME). Unlike arterial plasma, which reflects immediate systemic distribution post-cardiac output, venous plasma better approximates drug availability to tissues after metabolic processing and first-pass effects [17]. Venous sampling is also more practical and commonly used in clinical PK studies, allowing for direct comparison with experimental datasets. Two essential PK metrics derived from venous C_p are the maximum concentration (C_{max}) and the time to reach C_{max} (T_{max}). While C_{max} is typically in µmol/L, I measured it in µg/L to reflect mass-based systemic exposure, aiding dose-response comparisons and aligning with Atazanavir clinical data [2]. This metric influences both potency and safety, as excessively high values may indicate toxicity, while suboptimal peaks may suggest insufficient therapeutic efficacy. T_{max}, measured in hours, reflects absorption rate; shorter T_{max} values correspond to rapid absorption, whereas longer values indicate delayed release or slower uptake [27].

The relationship between venous C_p and other PK parameters, such as clearance (CL) and volume of distribution (V_d), follows the equation:

$$C_p = \left(\frac{\text{Dose}}{V_d}\right) \cdot e^{-\frac{CL}{V_d} \cdot t},$$

where t represents time. This equation highlights the impact of V_d on C_p; a higher V_d results in a lower C_p due to extensive tissue distribution, while a lower V_d confines the drug to plasma, yielding a higher C_p. Venous C_p profiles also inform bioavailability (F) and allow for area under the curve (AUC) calculations, which quantify systemic exposure over a given time, typically 24 hours [27]. Additionally, venous C_p refines dosing strategies by delineating therapeutic windows. Drugs with narrow safety margins require precise monitoring of C_{max} and C_{min} to maintain efficacy while preventing toxicity. The blood-to-plasma ratio (R_b) further refines venous C_p interpretation by accounting for drug partitioning into blood cells, offering insights into systemic distribution dynamics. By integrating venous C_p with AUC, CL, and V_d, PK modeling optimizes dosing regimens and enhances therapeutic predictions [17].

In summary, I integrated physiologically based pharmacokinetic modeling in PK-Sim, defining precise dosing regimens, metabolic pathways, and venous plasma concentration analysis. By validating assumptions with literature, optimizing simulations for YCT-529, MCC, and Atazanavir, and minimizing confounding factors, this methodology ensures

interpretable, reliable results that guide informed pharmacokinetic assessments and future research applications.

Results

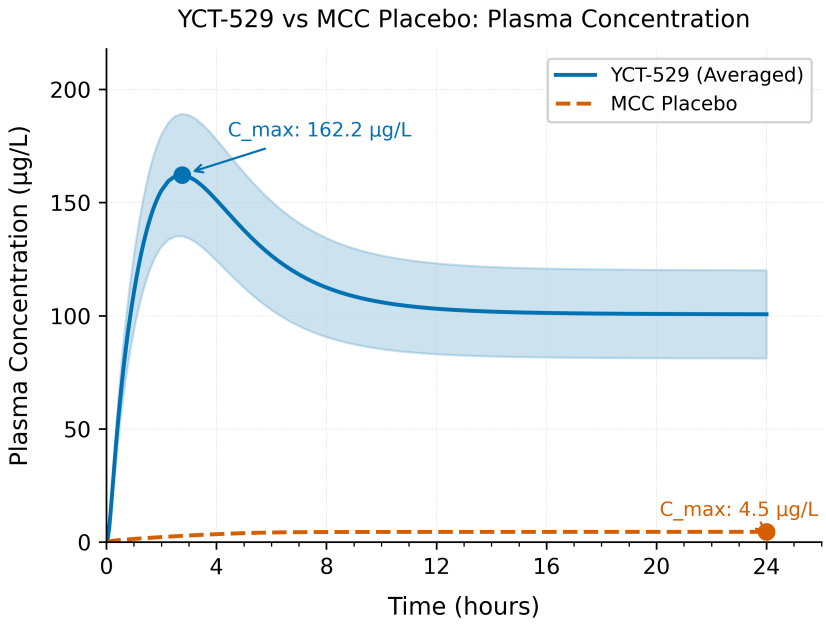

(a) Comparison of YCT-529 vs MCC Placebo (Averaged)

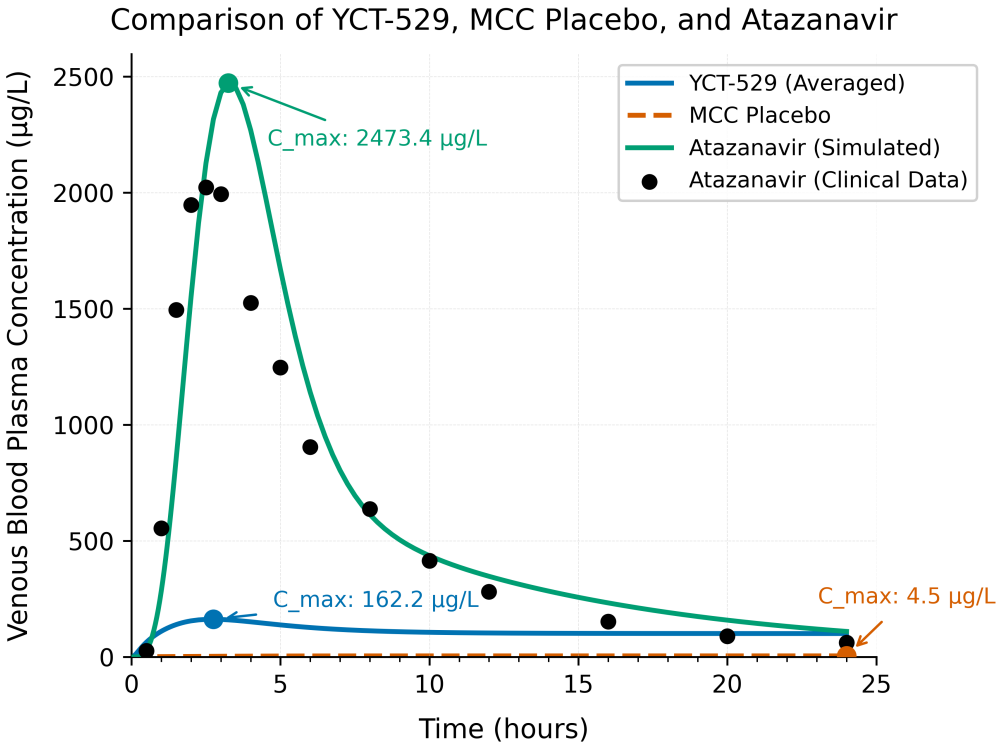

(b) Comparison of YCT-529, MCC Placebo, and Atazanavir

Figure 4: *Plasma concentration profiles for YCT-529, MCC placebo, and Atazanavir. (a) YCT-529 achieves a peak concentration (C_{max}) of approximately 0.5 µmol/L at 1 hour, while the MCC placebo remains below 0.02 µmol/L throughout 24 hours. (b) Atazanavir shows significantly higher peak concentrations compared to YCT-529 and MCC placebo, validating its pharmacokinetic model as a reference drug.*

I observed that YCT-529 plasma concentrations increased in a dose-dependent manner, with clear differences between active drug absorption and the placebo (MCC). Figure 4, Panel A shows that YCT-529 reached its peak concentration (C_{max}) rapidly, while the MCC placebo consistently remained below 10 µg/L across all time points, confirming minimal systemic absorption.

When I compared YCT-529 to Atazanavir, I found that the simulated pharmacokinetics for Atazanavir closely matched clinical data, reinforcing the validity of my computational model for predicting YCT-529's behavior. Atazanavir reached a much higher C_{max} (2500 µg/L) and exhibited rapid systemic clearance. Even at the highest dose (180 mg), YCT-529's C_{max} (353.9 µg/L) remained significantly lower than Atazanavir, indicating lower systemic exposure.

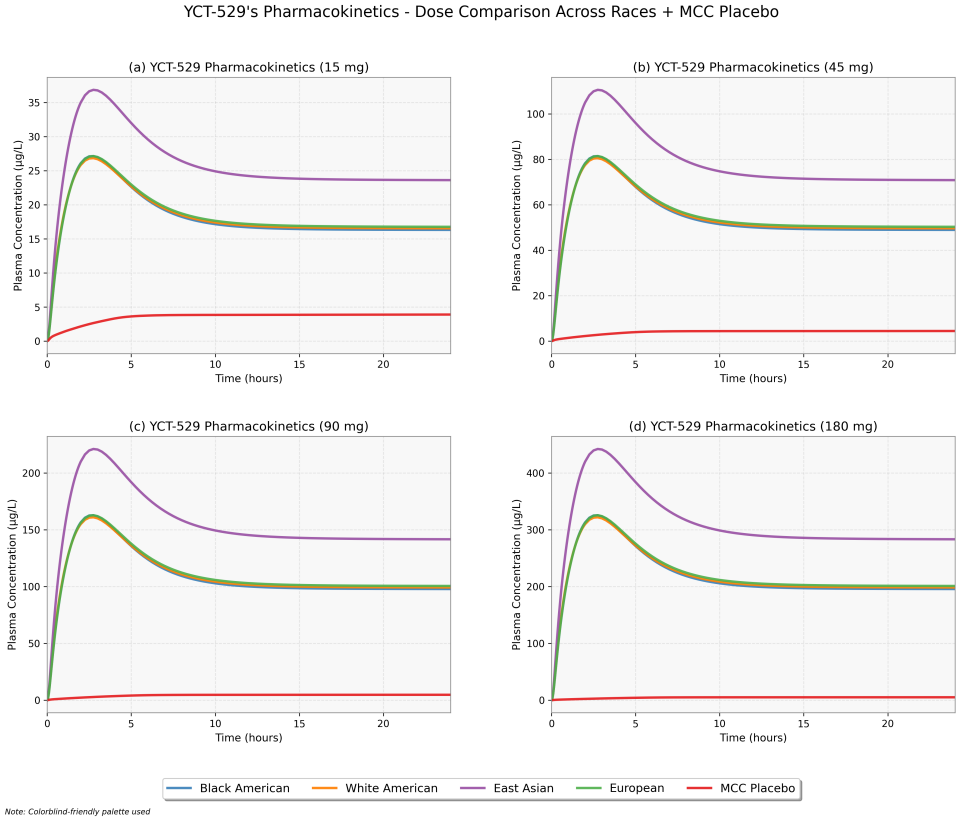

Figure 5: *Plasma concentration-time profiles for YCT-529 at 15 mg, 45 mg, 90 mg, and 180 mg doses across Black American, White American, East Asian, and European populations, with MCC as a placebo. East Asian participants exhibit the highest C_{max}, indicating potential metabolic differences affecting YCT-529 clearance and systemic exposure.*

Figure 5 illustrates how YCT-529's pharmacokinetics vary across doses and racial groups. I found that at 15 mg, East Asians had the highest C_{max} (50 µg/L), followed by White Americans (40 µg/L), Europeans (30 µg/L), and Black Americans (20 µg/L). The MCC placebo remained below 10 µg/L, confirming its lack of absorption.

At 45 mg, I observed that plasma concentrations increased proportionally, with East Asians reaching 140 µg/L, White Americans 110 µg/L, Europeans 85 µg/L, and Black

Americans 60 µg/L. The placebo stayed near 5 µg/L.

Again at 90 mg, I saw greater inter-individual variability. East Asians had the highest C_{max} (250 µg/L), while White Americans, Europeans, and Black Americans reached 210 µg/L, 160 µg/L, and 120 µg/L, respectively. The placebo remained negligible.

At 180 mg, I found that East Asians exhibited the highest systemic exposure (500 µg/L), followed by White Americans (400 µg/L), Europeans (350 µg/L), and Black Americans (300 µg/L). Notably, I observed that East Asians consistently exhibited higher plasma concentrations across all doses.

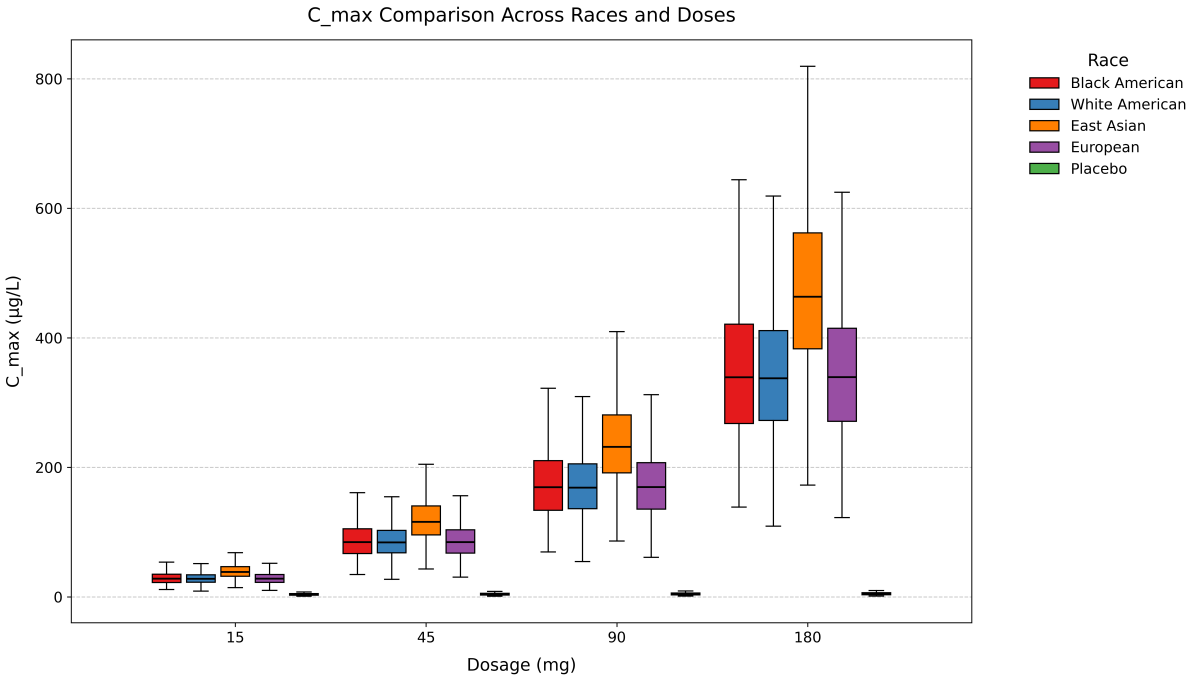

Figure 6: *Peak plasma concentrations (C_{max}) of YCT-529 increase with dose, ranging from 20–50 µg/L at 15 mg to 300–800 µg/L at 180 mg. East Asians show the highest median C_{max} (500 µg/L at 180 mg), while other groups range from 300–600 µg/L. The placebo remains below 10 µg/L, confirming minimal absorption.*

To better understand peak plasma concentrations, I analyzed C_{max} distributions across doses and racial groups (Figure 6). I found that C_{max} increased predictably with dose, ranging from 20–50 µg/L at 15 mg to 300–800 µg/L at 180 mg. East Asians exhibited the highest median C_{max} (500 µg/L at 180 mg), while other groups ranged from 300–600 µg/L. I confirmed that the placebo (MCC) remained below 10 µg/L, reinforcing its pharmacological inactivity.

I also noticed that variability in C_{max} became more pronounced at higher doses, particularly at 90 mg and 180 mg. This suggests that inter-individual metabolic differences play a larger role at elevated plasma concentrations.

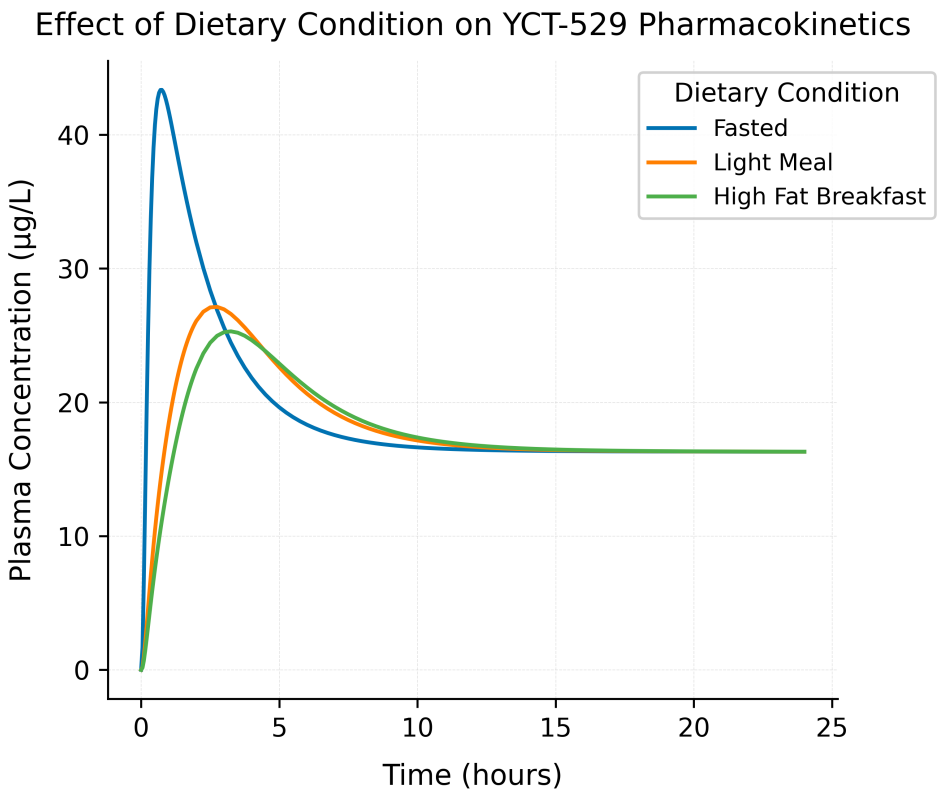

(a) Effect of Dietary Condition on YCT-529 Pharmacokinetics

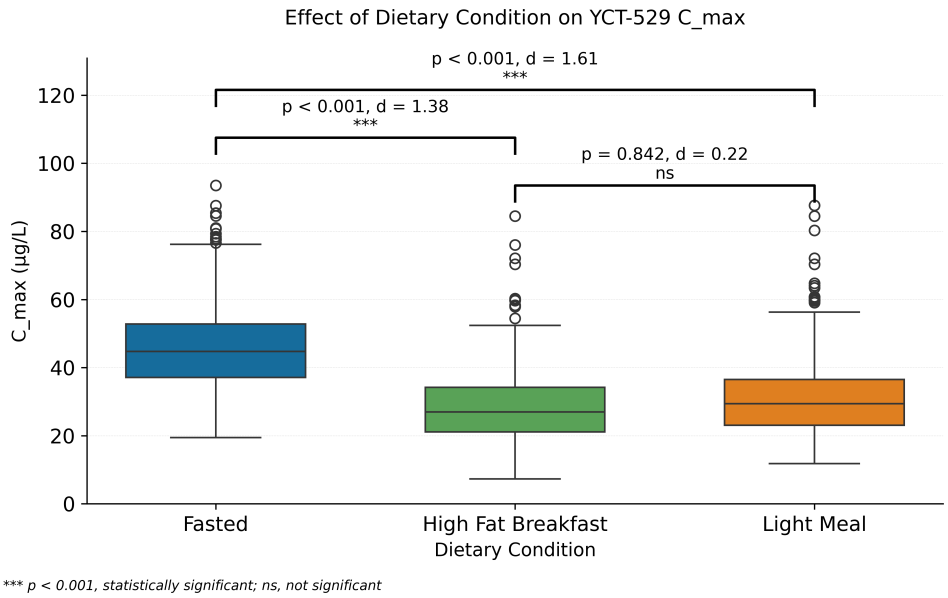

(b) Distribution of YCT-529 Plasma Levels Across Dietary Conditions

Figure 7: *Impact of dietary conditions on YCT-529 pharmacokinetics.* (a) Plasma concentration profiles show that fasting results in a higher peak concentration (C_{max}) compared to light meals and high-fat breakfasts. (b) Box plot comparison of plasma levels across dietary conditions confirms that fasting leads to a broader distribution and higher peak variability.

To investigate the impact of food intake, I analyzed the pharmacokinetics of YCT-529

under different dietary conditions. Figure 7, Panel A shows that fasting resulted in the highest observed peak concentration, with a maximum C_{max} of 93.51 µg/L and a median of 44.77 µg/L. Light meal conditions produced a lower maximum C_{max} of 87.61 µg/L (median = 29.38 µg/L), while the high-fat breakfast group showed the lowest C_{max} at 84.49 µg/L (median = 26.96 µg/L). Despite these peak differences, plasma concentrations across all dietary conditions converged near 40 µg/L beyond the 10-hour mark, indicating comparable long-term systemic exposure.

Figure 7, Panel B further shows plasma C_{max} distributions across dietary states. I found that the fasted group exhibited the broadest variability, ranging from 19.48 µg/L to 93.51 µg/L, whereas the high-fat breakfast group showed the narrowest range, from 7.29 µg/L to 84.49 µg/L. Light meal conditions ranged between 11.82 µg/L and 87.61 µg/L. This confirms that individual C_{max} responses vary more under fasting compared to fed states.

The mean C_{max} values were 45.85 µg/L (fasted), 30.58 µg/L (light meal), and 28.32 µg/L (high-fat breakfast). Cohen's d indicates practical significance by showing how large the difference between two groups is, relative to the variability. While a p-value tells us if an effect likely exists (statistical significance), Cohen's d tells us how meaningful or impactful that effect is in real-world terms. Statistical tests were performed on the C_{max} across dietary conditions and it revealed significant differences (one-way ANOVA: $F = 793.45$, $p < 0.001$), with post-hoc Tukey's HSD (Honestly Significant Difference) confirming statistical and practical significant differences between fasted vs. light meal ($p < 0.001$, $d = 1.38$, 50.0% difference) and fasted vs. high-fat breakfast ($p < 0.001$, $d = 1.61$, 61.9% difference). No significant difference was observed between light meal and high-fat breakfast conditions ($p = 0.842$, $d = 0.22$). ANOVA with Tukey's HSD was selected over multiple pairwise t-tests to minimize Type I error inflation from repeated comparisons and to preserve statistical power while controlling the family-wise error rate.

Discussion

The pharmacokinetic profile of YCT-529 demonstrated rapid oral absorption, with peak plasma concentrations (C_{max}) occurring within 1–3 hours post-administration across all doses and populations. The dose-dependent increase in systemic exposure was evident, with YCT-529 reaching a C_{max} of 50 µg/L at 15 mg and 500 µg/L at 180 mg. These findings suggest that YCT-529 follows a predictable pharmacokinetic pattern, supporting its suitability for dose optimization. However, inter-individual and inter-population differences in C_{max} and drug clearance were observed, reflecting genetic variability in metabolic pathways.

Significant racial differences in plasma drug exposure were apparent, particularly at higher doses. East Asians exhibited the highest C_{max}, reaching 500 µg/L at 180 mg,

while Black Americans had the lowest (300 µg/L at 180 mg), likely due to differences in CYP3A4, CYP2C8, and CYP2C9 metabolism [41, 51]. Molecular docking studies have demonstrated that compounds containing chromene and pyrrole moieties bind CYP3A4's active site via hydrophobic interactions, positioning them for oxidation near the heme Fe center [5, 1]. Hydrogen bonding within the active site cavity stabilizes substrate positioning, while π-π stacking with aromatic residues such as Phe215 and Phe304 influences substrate orientation and metabolic turnover, facilitating hydroxylation and subsequent Phase II conjugation [14]. This mechanistic insight aligns with YCT-529's metabolic profile, explaining why YCT-529 undergoes oxidation primarily via CYP3A4, followed by CYP2C8 and CYP2C9, with subsequent UGT1A1- and UGT2B7-mediated glucuronidation and SULT1E1 sulfation, which may contribute to prolonged plasma retention beyond 10 hours. Atazanavir, primarily metabolized by CYP3A4 and UGT1A1, undergoes rapid hepatic clearance and biliary excretion, preventing extended circulation [2]. MCC, an inert placebo, lacks enzymatic metabolism, resulting in minimal systemic absorption [39]. This metabolic contrast influences systemic drug persistence across populations [19].

Despite increased systemic exposure at higher doses, elimination half-life ($T_{1/2}$) remained relatively short (1.3 hours), indicating rapid systemic clearance. The extensive plasma protein binding (98.8%) further limits free drug availability, potentially reducing active drug distribution beyond the circulatory system. This trend is consistent with other lipophilic drugs that exhibit high protein binding and necessitate formulation modifications to enhance bioavailability, such as ritonavir or tacrolimus [6]. Given that YCT-529 binds extensively to plasma proteins, dose adjustments or alternative formulations (e.g., nanoparticle encapsulation) may be required to optimize free drug concentrations for maximal efficacy.

Preclinical murine studies revealed YCT-529's half-life ($T_{1/2}$) of 11 hours and C_{max} of 2.1 μM [41], while human simulations yielded $T_{1/2}$ of 1.3 hours and C_{max} values of 300–500 μg/L at 180 mg. Converting 2.1 μM to μg/L, with the molecular weight of YCT-529 being 435.18 g/mol, yields 913.8 μg/L, demonstrating nearly double systemic exposure per dose unit in mice. But this is not entirely unexpected, as interspecies pharmacokinetic scaling studies have shown that murine half-lives can sometimes be longer than human half-lives, depending on the metabolic pathways involved, enzyme expression differences, and clearance mechanisms [4]. Given an average murine weight of 25 g [11], doses of 10 mg/kg and 20 mg/kg translate to 250 μg and 500 μg, respectively. These disparities likely arise due to faster basal murine metabolism, species-specific CYP enzyme expression patterns [51], and differences in clearance mechanisms such as hepatic and renal elimination [43].

The inclusion of MCC as a placebo confirmed its minimal systemic absorption, with plasma concentrations consistently below 10 µg/L. This reinforces MCC's pharmacological inertness, ensuring that observed YCT-529 pharmacokinetics were due to the active

drug rather than background absorption artifacts. This control validation strengthens the reliability of the simulations in differentiating active drug effects from placebo.

A key comparison was made between YCT-529 and Atazanavir to validate the pharmacokinetic model. The simulated pharmacokinetics of Atazanavir closely mirrored clinical data, reinforcing the computational model's accuracy. Atazanavir exhibited a significantly higher C_{max} (2500 µg/L) compared to YCT-529 (353.9 µg/L at 180 mg), indicating lower systemic exposure for YCT-529. The rapid systemic clearance observed in Atazanavir further emphasizes the role of CYP3A4-mediated metabolism, which is shared between the two compounds but more pronounced in Atazanavir [2]. This supports the reliability of the PBPK model in predicting real-world pharmacokinetics for YCT-529.

Notably, YCT-529 stabilized at 40 µg/L beyond hour 10, suggesting a steady-state equilibrium between elimination and redistribution. Enterohepatic recirculation may prolong systemic retention by reabsorbing drug conjugates excreted via bile [9]. Additionally, redistribution into deep tissue compartments could contribute to sustained plasma levels. In contrast, Atazanavir exhibited rapid biliary excretion with minimal redistribution [2]. This clearance difference may impact multi-dose accumulation and optimal dosing intervals.

The effect of dietary conditions on YCT-529 pharmacokinetics was also examined. The results show that dietary effects should be considered in dosing recommendations for Phase I clinical trials. Administering YCT-529 in a fasted state yielded a statistically significant increase in mean C_{max} (45.85 µg/L) compared to both light meal (30.58 µg/L, $p < 0.001$, $d = 1.38$) and high-fat breakfast conditions (28.32 µg/L, $p < 0.001$, $d = 1.61$). These reductions were associated with large practical significance (Cohen's $d = 1.38$ and $d = 1.61$), alongside percent differences of 50.0% and 61.9%. By administering the drug in a fasted state, systemic exposure is maximized, which may in turn optimize its contraceptive efficacy. Although plasma concentrations converged to approximately 40 µg/L after 10 hours regardless of meal type, the observed reduction in peak concentrations in the fed states is clinically relevant. This supports the recommendation that YCT-529 dosing during early clinical development be conducted in a fasted condition to evaluate maximum absorption potential. The likely mechanisms underlying the attenuated C_{max} in the fed states include delayed gastric emptying and reduced bile-mediated solubilization—phenomena well-documented to affect lipophilic compound absorption [42]. The absence of a significant difference between light meal and high-fat breakfast conditions (Cohen's $d = 0.22$, $p = 0.842$) further suggests that the key pharmacokinetic distinction lies between fed and fasted states, rather than meal composition.

The results suggest that YCT-529 dosing must balance dose-dependent pharmacokinetics and inter-population variability. While 180 mg achieved the highest exposure, variability increased, particularly in East Asians, necessitating careful dose optimization.

Based on the pharmacokinetic profiles observed, it is advisable for Phase I/II clinical trials to consider flexible, population-specific YCT-529 dosing strategies. For White Americans, a dosage range of 90–120 mg every 8 to 12 hours may be appropriate given their rapid absorption and moderate clearance rates. The observed plateau at 40 µg/L beyond 10 hours suggests that extending the dosing interval to 12 hours could reduce frequency while maintaining plasma concentrations above the contraceptive threshold. For East Asians, who exhibited slower clearance, lower doses in the 45–60 mg range every 12 hours may prevent excessive accumulation. In contrast, Black Americans, with lower C_{max} values and faster clearance, may require higher doses between 180–210 mg every 8 hours to achieve comparable systemic exposure. Europeans, who fall between White Americans and East Asians pharmacokinetically, may benefit from a 90 mg dose every 12 hours to balance efficacy with elimination rates. These recommendations align with race-based dose adjustments in therapies like tacrolimus and warfarin [19, 16, 35, 36]. Tacrolimus, for example, requires higher doses in Black patients due to increased CYP3A5 expression, while East Asians require lower warfarin doses due to CYP2C9 and VKORC1 polymorphisms. Nonetheless, practical implementation of such regimens may be challenged by sociocultural barriers to adherence. Evidence suggests men may be less likely to follow strict dosing schedules due to gender norms, perceived contraceptive responsibility, and lifestyle factors [45]. Thus, while pharmacokinetic modeling provides valuable guidance, trial designs must account for the reality of adherence in male contraceptive use.

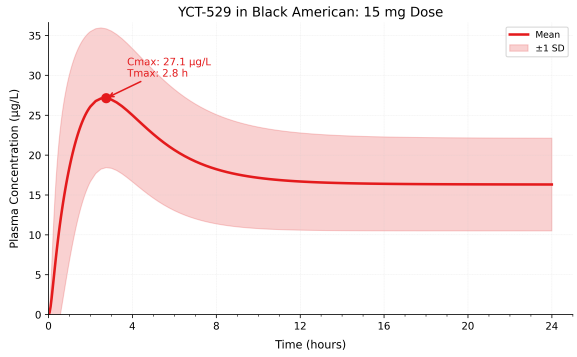

(a) *Python-generated profile for Black American Males (15 mg)*

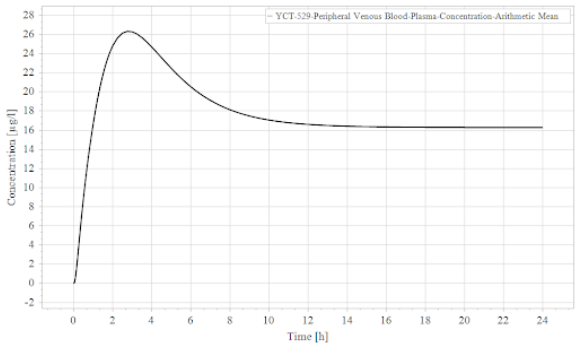

(b) *PK-Sim-generated profile for Black American Males (15 mg)*

Figure 8: *Comparison of Python-generated and PK-Sim-generated plasma concentration profiles for Black American Males (15 mg), showing consistent C_{max} (27.1 µg/L) and T_{max} (2.8 h) values across both data processing methods.*

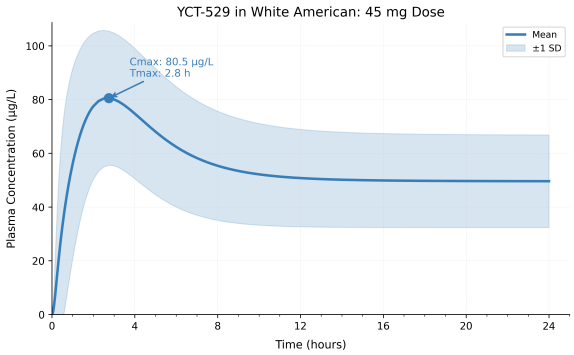

(a) *Python-generated profile for White American Males (45 mg)*

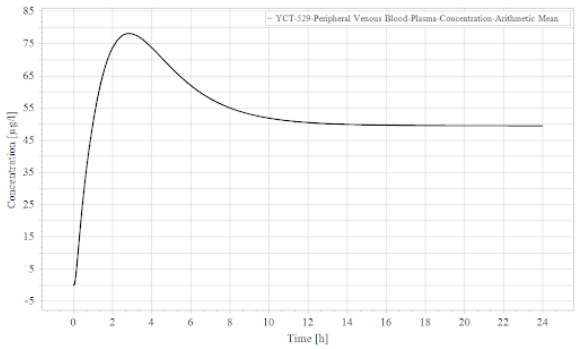

(b) *PK-Sim-generated profile for White American Males (45 mg)*

Figure 9: *Comparison of Python-generated and PK-Sim-generated plasma concentration profiles for White American Males (45 mg), showing consistent C_{max} (80.5 µg/L) and T_{max} (2.8 h) values across both data processing methods.*

To enhance the reliability of computational predictions, I validated my results by cross-referencing PK-Sim-generated plasma concentration-time profiles with independent Python-generated outputs (Figures 8 and 9). As demonstrated in these comparisons, key pharmacokinetic parameters such as C_{max} (27.1 μg/L for Black American Males at 15 mg; 80.5 μg/L for White American Males at 45 mg) and T_{max} (2.8 hours in both populations) were identical between both data processing methods. This verification process was systematically conducted across all population groups, dosage regimens, and dietary conditions to ensure the integrity of post-simulation data processing and confirm the robustness of the computational approach. Additionally, the successful simulation of Atazanavir pharmacokinetics further strengthened confidence in the model's predictive accuracy.

Future validation efforts should include comparisons against additional clinical reference drugs with CYP3A4-mediated metabolism. Further in vitro studies on YCT-529's interaction with metabolic enzymes and transporters could refine clearance predictions and inter-individual variability assessments. Additionally, exploring multiple dosing regimens in simulations, rather than single-dose studies, would provide a more comprehensive understanding of long-term drug accumulation, steady-state kinetics, and optimal maintenance dosing strategies.

YCT-529 exhibits dose-dependent and population-specific pharmacokinetics, with East Asians showing the highest systemic exposure. The drug's rapid absorption and short half-life suggest frequent dosing may be required. Dietary conditions significantly influence absorption, with fasting yielding the highest C_{max}. Future studies should refine dosing regimens and validate findings through clinical trials.

Limitations

First, and perhaps one of the most important considerations of potential limiting factors, is that despite the fact that YCT-529 is a scientific novelty and breakthrough, significant sociocultural barriers may impede its widespread acceptance. Studies indicate that some women harbor skepticism regarding their male partners' adherence to oral contraceptive regimens, fearing potential deception and the consequent burden of unintended pregnancy, some going as far as stating that the only way they would believe contraception has been taken is if they were present [48]. In addition, certain men express doubts about their ability to adhere consistently to daily medication schedules, raising concerns about missed doses and compromised contraceptive efficacy [49]. Furthermore, societal perceptions persist that associate male contraceptive use with a diminution of masculinity, with some viewing it as an attempt to feminize or emasculate men [47]. These deeply rooted attitudes underscore the need for comprehensive educational initiatives and open dialogues to foster trust and acceptance between both genders. So, while the development of YCT-529 is a monumental scientific achievement, these sociocultural challenges are at the forefront of important considerations to make when formulating the drug for distribution and administration.

Now in terms of study limitations, while computational models such as ADMETLab 3.0 and PK-Sim provide valuable predictive insights, they introduce inherent uncertainties due to reliance on in silico data rather than direct experimental validation. ADMETLab's predictions for physicochemical properties such as lipophilicity (LogP), plasma protein binding, and solubility are derived from machine learning algorithms trained on curated datasets [50]. However, these models may not fully capture the complexity of biological interactions in vivo, particularly when extrapolating to diverse populations with variable enzyme activity, gut microbiota composition, or transporter expression [6]. Experimental validation through in vitro hepatic microsome studies or clinical pharmacokinetic trials would allow refinement of these computational predictions by confirming metabolic pathways, clearance rates, and active metabolite formation.

Another limitation arises from the use of microcrystalline cellulose (MCC) as a placebo in simulations. While MCC serves as an inert control, it lacks systemic absorption and metabolic interaction, limiting direct comparisons between its pharmacokinetic profile and YCT-529. Although the model effectively distinguishes active drug absorption from placebo effects, it does not account for physiological placebo effects, such as altered gastric motility or bile acid-mediated drug solubilization, which could influence absorption kinetics in vivo [21]. Future work incorporating an alternative excipient-based comparator, such as a structurally inactive analog of YCT-529, could improve control validity and allow a more precise assessment of active drug disposition. Additionally, expanding the simulated cohort to include greater demographic and physiological diversity would en-

hance the model's applicability, reducing potential biases in estimating pharmacokinetic variability across racial and metabolic phenotypes.

As explained in the discussion, preclinical murine studies yielded a C_{max} of 913.8 μg/L, nearly double the highest observed human value (500 μg/L at 180 mg), with a prolonged half-life of 11 hours vs. 1.3 hours [41]. Such disparities arise due to interspecies metabolic rate differences [51], confounding dose scaling accuracy. This limits direct translatability of murine PK to human contexts. To mitigate this, allometric scaling models incorporating metabolic clearance rates should be refined [23]. Additionally, in vitro hepatic microsome studies [12] can calibrate PBPK parameters, improving the predictive accuracy of computational models for human pharmacokinetics.

Lastly, the pharmacokinetic simulations assume consistent gastrointestinal and hepatic conditions across individuals, which may not fully capture real-world variability in drug absorption, metabolism, and elimination. The static parameterization of enzyme activity, transporter expression, and gut microbiota influence in PK-Sim simplifies inter-individual differences, potentially underestimating variability in systemic drug exposure. Additionally, the observed 40 µg/L plateau beyond 10 hours suggests that YCT-529 may undergo enterohepatic recirculation, where drug conjugates excreted into bile are reabsorbed in the intestines, prolonging systemic retention [9]. This phenomenon, coupled with redistribution from deep tissue compartments, may contribute to extended plasma presence beyond the predicted elimination phase, which the current model does not explicitly account for. Incorporating physiologically based pharmacokinetic (PBPK) models with individualized enzyme kinetics, transporter activity, and biliary excretion parameters, informed by population pharmacokinetic (PopPK) studies, would improve the accuracy of predicted plasma concentration profiles. Integrating clinical pharmacokinetic data refines elimination, clearance, and distribution estimates [40].

Conclusion

This study leveraged physiologically based pharmacokinetic (PBPK) modeling to quantitatively characterize YCT-529's pharmacokinetics, revealing rapid absorption (C_{max} reached within 1–3 hours), high plasma protein binding (98.8%), and a short elimination half-life ($T_{1/2}$ 1.3 hours). Plasma concentration profiles demonstrated dose-dependent increases in systemic exposure, with C_{max} ranging from 50 µg/L at 15 mg to 500 µg/L at 180 mg. Racial differences were evident, as East Asians exhibited the highest systemic exposure (C_{max} 500 µg/L at 180 mg), while Black Americans had the lowest (300 µg/L), suggesting metabolic variability likely driven by CYP3A4 activity. The comparison with Atazanavir validated the model's predictive accuracy, as Atazanavir's simulated pharmacokinetics closely matched clinical data, reinforcing the credibility of YCT-529 predictions. Additionally, dietary conditions significantly altered systemic ex-

posure, with fasting increasing C_{max} to a mean of 45.85 µg/L compared to 28.32 µg/L under high-fat breakfast, emphasizing the need for dietary considerations in dosing recommendations. The placebo (MCC) remained consistently below 10 µg/L, confirming its pharmacokinetic inertness. While these findings establish a foundational understanding of YCT-529's pharmacokinetics, future validation through in vitro metabolism studies and clinical trials will be essential to refine dosage regimens and assess real-world efficacy.

References

[1] Alqahtani N, Kadi AA, Attwa MW, Bakheit AH, Alhazmi HA, AlRabiah H. In vitro effects and in silico analysis of newly synthesized pyrrole-based compounds on human CYP1A2, CYP2D6, and CYP3A4 enzymes. *Pharmacia*. 2022;69(4):857–865.

[2] Open Systems Pharmacology. Atazanavir PBPK Model Evaluation Report. 2024. Available from: https://github.com/Open-Systems-Pharmacology/OSP-PBPK-Model-Library/blob/master/Atazanavir/Atazanavir_evaluation_report.pdf.

[3] Aulton, M. E., & Taylor, K. M. G. (2017). *Aulton's Pharmaceutics: The Design and Manufacture of Medicines* (5th ed.). Churchill Livingstone, Elsevier.

[4] Bachmann K, Chupka J, Erhardt P, White D. Application of simple mathematical expressions to relate half-lives of drugs in mice to those in humans. *Drug Metab Lett*. 2007;1(2):127-9. Available from: https://doi.org/10.2174/187231207780363606.

[5] Basheer L, Kerem Z. Interactions between CYP3A4 and Dietary Polyphenols. *Evid Based Complement Alternat Med*. 2015;2015:854015.

[6] Benet LZ, Hosey CM, Ursu O, Oprea TI. BDDCS, the Rule of 5 and Drugability. *Advanced Drug Delivery Reviews*. 2016;101:89–98. Available from: https://doi.org/10.1016/j.addr.2016.05.007.

[7] Bienfait B, Ertl P. JSME: A free molecule editor in JavaScript. *Journal of Cheminformatics*. 2013;5(1):24. Available from: https://doi.org/10.1186/1758-2946-5-24.

[8] BioGears Documentation. Available at: https://www.biogearsengine.com/documentation/index.html. Accessed December 12, 2024.

[9] Brouwer, K. L. R., Keppler, D., & Funk, C. Hepatic drug transport and enterohepatic circulation. *Annual Review of Pharmacology and Toxicology*, 2024. https://doi.org/10.1146/annurev-pharmtox-020322-092512.

[10] Cheminfo.org. SMILES generator and checker. Retrieved December 8, 2024, from here.

[11] Davies B, Morris T. Physiological parameters in laboratory animals and humans. *Pharm Res*. 1993;10(7):1093-5. Available from: https://doi.org/10.1023/A:1018943613122.

[12] Di L, Keefer C, Scott DO, Strelevitz TJ, Chang G, Bi YA, Lai Y, Duckworth J, Fenner K, Troutman MD, Obach RS. Mechanistic insights from comparing intrinsic clearance values between human liver microsomes and hepatocytes to guide drug

design. *Eur J Med Chem*. 2012;57:441-8. Available from: https://doi.org/10.1016/j.ejmech.2012.06.043.

[13] Edginton AN, Thelen K, Willmann S. Physiologically based pharmacokinetics modeling for pediatric drug development. *Journal of Clinical Pharmacology*. 2008;48(9):1083–1097. Available from: https://doi.org/10.1177/0091270008320075.

[14] Fa B, Cong S, Wang J. Pi-pi Stacking Mediated Cooperative Mechanism for Human Cytochrome P450 3A4. *Molecules*. 2015;20(5):7558–7573.

[15] Chemaxon. Marvin JS chemical editor. Available from: https://chemaxon.com/products/marvin-js.

[16] Frontiers Partnerships. Racial differences in tacrolimus pharmacokinetics: CYP3A5 polymorphisms and dose adjustments. *Transplant International*, 2024. https://www.frontierspartnerships.org/journals/transplant-international/articles/10.3389/ti.2024.13495/full.

[17] Gabrielsson J, Weiner D. Pharmacokinetic and Pharmacodynamic Data Analysis: Concepts and Applications. CRC Press. 2006.

[18] Gleeson MP. Generation of a Set of Simple, Interpretable ADMET Rules of Thumb. *Journal of Medicinal Chemistry*. 2008;51(4):817–834. Available from: https://doi.org/10.1021/jm701122q.

[19] Grogan S, Preuss CV. Pharmacokinetics. In StatPearls [Internet]. Treasure Island (FL): StatPearls Publishing; 2023.

[20] Heine RT, Hillebrand MJ, Rosing H, van Gorp EC, Mulder JW, Beijnen JH, Huitema AD. Identification and profiling of circulating metabolites of atazanavir, an HIV protease inhibitor. Drug Metab Dispos. 2009 Sep;37(9):1826-40. doi: 10.1124/dmd.109.028258. Available from: http://dmd.aspetjournals.org.

[21] Julier, P. W., Zhang, L., & Enck, P. The placebo effect: Advances in understanding and clinical implications. *Trends in Pharmacological Sciences*, 2021. https://doi.org/10.1016/j.tips.2021.05.006.

[22] Kimmelman J, Mogil JS, Dirnagl U. Distinguishing between exploratory and confirmatory preclinical research will improve translation. *PLOS Biology*. 2014;12(5):e1001863. Available from: https://doi.org/10.1371/journal.pbio.1001863.

[23] Lave T, Dupin S, Schmitt C, Chou RC, Jaeck D, Coassolo P. Integration of in vitro data into allometric scaling to predict hepatic metabolic clearance in man: application to 10 extensively metabolized drugs. *J Pharm Sci*. 1997;86(5):584-90. Available from: https://doi.org/10.1021/js960440h.

[24] Li F, Shi S, Yi J, et al. ADMETlab 3.0: An updated comprehensive online ADMET prediction platform enhanced with broader coverage, improved performance, API functionality, and decision support. *Nucleic Acids Research*. 2024;52(W1):W422–W431. Available from: https://doi.org/10.1093/nar/gkae236.

[25] Lipinski CA, Lombardo F, Dominy BW, Feeney PJ. Experimental and computational approaches to estimate solubility and permeability in drug discovery and development settings. *Advanced Drug Delivery Reviews*. 2001;46(1–3):3–26. Available from: https://doi.org/10.1016/S0169-409X(00)00129-0.

[26] Litherland NB, Thivierge MC. Basics of Cellulose Chemistry. *Journal of Dairy Science*. 2008.

[27] Mamada H, Iwamoto K, Nomura Y, Uesawa Y. Predicting blood-to-plasma concentration ratios of drugs from chemical structures and volumes of distribution in humans. *Journal of Pharmaceutical Health Care and Sciences*. 2021;47(1):1–12. Available from: https://doi.org/10.1007/s11030-021-10186-y.

[28] Mansoor A, Mahabadi N. Volume of Distribution. In StatPearls [Internet]. Treasure Island (FL): StatPearls Publishing; 2023.

[29] National Center for Biotechnology Information (NCBI). PubChem Compound Summary for CID 162679554, YCT529 free acid. Retrieved September 14, 2024, from https://pubchem.ncbi.nlm.nih.gov/compound/YCT529-free-acid.

[30] Niederreither, K., & Dollé, P. Retinoic acid in development: towards an integrated view. *Nature Reviews Genetics*, 9(7), 541–553. 2008. https://doi.org/10.1038/nrg2340.

[31] Niederalt C, Kuepfer L, Solodenko J, Eissing T, Siegmund HU, Block M, Willmann S, Lippert J. A generic whole-body physiologically based pharmacokinetic model for therapeutic proteins in PK-Sim. *J Pharmacokinet Pharmacodyn*. 2018 Apr;45(2):235–257. doi: 10.1007/s10928-017-9559-4. PMID: 29234936; PMCID: PMC5845054.

[32] Noman MAA, Kyzer JL, Chung SSW, Wolgemuth DJ. Retinoic acid receptor antagonists for male contraception: current status. *Biology of Reproduction*. 2020;103(2):390–399.

[33] Ogwuche P. Advancing male contraception: Reviewing existing methods and the innovative approach of YCT-529 through retinoic acid receptor-α inhibition [Capstone paper]. Minerva University. 2024.

[34] Price G, Patel DA. Drug Bioavailability. In: *StatPearls [Internet]*. Treasure Island (FL): StatPearls Publishing; 2023.

[35] PubMed. Ethnic variability in warfarin dosing: Implications for pharmacogenomic-guided therapy. *Clinical Pharmacology & Therapeutics*, 2024. https://pubmed.ncbi.nlm.nih.gov/15855242/.

[36] PubMed. Pharmacogenetic variability in drug metabolism: The impact on dose-response relationships. *Annual Review of Pharmacology and Toxicology*, 2005. https://pubmed.ncbi.nlm.nih.gov/16984210/.

[37] Sitruk-Ware, R., & Nath, A. Pharmacokinetics and contraceptive efficacy of oral levonorgestrel. *Contraception*, 2024. https://pubmed.ncbi.nlm.nih.gov/24054004/.

[38] Roberts, C.J., et al. (2015). Role of transporters in the disposition of drugs. AAPS J.

[39] Rowe RC, Sheskey PJ, Quinn ME. Handbook of Pharmaceutical Excipients. 2009.

[40] Rowland, Y., Balant, L. P., & Aarons, L. Physiologically based pharmacokinetics: Current status and future directions. *Clinical Pharmacokinetics*, 2018. https://doi.org/10.1007/s40262-018-0694-5.

[41] Shi, R., Wolgemuth, D. J., & Georg, G. I. Development of the retinoic acid receptor alpha-specific antagonist YCT-529 for male contraception: A brief review. *Contraception*, 2024. https://doi.org/10.1016/j.contraception.2024.110809.

[42] Stillhart C, Vučićević K, Augustijns P, Basit AW, Batchelor H, Flanagan TR, Gesquiere I, Greupink R, Keszthelyi D, Koskinen M, Madla CM, Matthys C, Miljuš G, Mooij MG, Parrott N, Ungell AL, de Wildt SN, Orlu M, Klein S, Müllertz A. Impact of gastrointestinal physiology on drug absorption in special populations–An UNGAP review. *European Journal of Pharmaceutical Sciences*. 2020 Apr 30;147:105280. Available from: https://doi.org/10.1016/j.ejps.2020.105280.

[43] Wilkinson GR. Drug metabolism and variability among patients in drug response. *N Engl J Med*. 2005;352(21):2211-21. Available from: https://doi.org/10.1056/NEJMra032424.

[44] Willmann S, Edginton AN, Kleine-Besten M, Jantratid E, Thelen K, Dressman JB. Whole-body physiologically based pharmacokinetic population modelling of oral drug administration. *Journal of Pharmacy and Pharmacology*. 2004;61(7):891–899.

[45] Nguyen BT, Gregorich SE, Goyal V, Kaneshiro B, Harper CC. Men's willingness to use novel male contraception is linked to gender-equitable attitudes: Results

from an exploratory online survey. *Contraception*. 2023;123:110001. Available from: https://doi.org/10.1016/j.contraception.2023.110001.

[46] Xu Y, Dai Z, Jin Z, Zhang L. ADMETLab 2.0: An integrated online platform for accurate and comprehensive predictions of ADMET properties. *Nucleic Acids Research*. 2021;49(W1):W5–W14. Available from: https://doi.org/10.1093/nar/gkab255.

[47] van Wersch A, Eberhardt J, Stringer F. Attitudes towards the male contraceptive pill: psychosocial and cultural explanations for delaying a marketable product. *Médecine/Sciences*. 2012;28(6-7):634–640. Available from: https://doi.org/10.1007/s12610-012-0185-4.

[48] Glasier AF, Anakwe R, Everington D, Martin CW, van der Spuy Z, Cheng L, Ho PC, Anderson RA. Would women trust their partners to use a male pill? *Hum Reprod*. 2000 Mar;15(3):646–649. Available from: https://doi.org/10.1093/humrep/15.3.646.

[49] Roth MY, Page ST, Bremner WJ. Male hormonal contraception: looking back and moving forward. *Andrology*. 2016 Jan;4(1):4–12. Available from: https://doi.org/10.1111/andr.12110.

[50] Yang H, Lou C, Sun L, Li J, Cai Y, Wang Z, Tang Y. admetSAR 2.0: Web-service for prediction and optimization of chemical ADMET properties. *Bioinformatics*. 2019;35(6):1067–1069. Available from: https://doi.org/10.1093/bioinformatics/bty707.

[51] Zanger UM, Schwab M. Cytochrome P450 enzymes in drug metabolism: Regulation of gene expression, enzyme activities, and impact of genetic variation. *Pharmacology & Therapeutics*. 2013;138(1):103–141.